606 *Inorg. Chem.* **2010**, *49*, 606–615
DOI: 10.1021/ic901757u

Inorganic Chemistry
Article

Unsymmetrical Tripodal Ligand for Lanthanide Complexation: Structural, Thermodynamic, and Photophysical Studies

Badr El Aroussi,[†] Nathalie Dupont,[‡] Gérald Bernardinelli,[§] and Josef Hamacek*[,†]

[†]*Department of Inorganic, Analytical and Applied Chemistry,* [‡]*Department of Physical Chemistry, University of Geneva, 30 quai E. Ansermet, 1211 Geneva 4, Switzerland, and* [§]*Laboratory of X-ray Crystallography, University of Geneva, 24 quai E. Ansermet, 1211 Geneva 4, Switzerland*

Received September 3, 2009

Two tridentate and one bidentate binding strands have been anchored on a carbon atom to provide a new unsymmetrical tripodal ligand **L** for Ln(III) coordination. The ligand itself adopts a single conformation in solution stabilized by intramolecular hydrogen bonds evidenced in the solid state. The reaction of **L** with trivalent lanthanides provides different coordination complexes depending on the metal/ligand ratio. The speciation studies with selected lanthanides were performed in solution by means of NMR, ESMS, and spectrophotometric titrations. Differences in coordination properties along the lanthanide series were evidenced and may be associated with the changes in the ionic size. However, thermodynamic stability constants for the species of the same stoichiometry do not significantly vary. In addition, the structure of the dinuclear complex $[Eu_2\mathbf{L}_2]^{6+}$ has been elucidated in the solid state, where the complex crystallizes predominantly as an *M*-isomer. The crystal structure shows the coordination of two different ligands to each europium cation through tridentate strands, and the europium nine-coordinate sphere is completed with three solvent molecules. Finally, the results of photophysical investigations of $[Eu_2\mathbf{L}_2]^{6+}$ are in close agreement with the structural parameters determined by crystallography.

Introduction

A considerable progress in the field of lanthanide chemistry has been stimulating the permanent interest of the scientific community in Ln(III)-containing compounds. Nevertheless, exploring lanthanide peculiar photophysical and paramagnetic properties still remains challenging for applications in sensors and biological assays (VIS and IR luminescence,[1] MRI imaging[2]). Such applications require the use of stable complexes to resist in an intricate environment of biological samples. Although a variety of ligands (mostly polyaminocarboxylates and macrocyclic derivatives) forming thermodynamically and kinetically stable complexes is already used in practice, the synthesis and development of new supramolecular systems may lead to a further enhancement of sensing efficiency. Generally, the choice of the appropriate ligand is crucial and predetermines most properties related to the final metal-containing assembly. In case of lanthanide complexes, the presence of a multidentate coordination cavity to satisfy lanthanide preferences for high coordination numbers is desired for ensuring sufficient thermodynamic stability.[3] In this context, a significant effort was devoted to the investigation of complexes with tripodal ligands. The formation of such tripodal complexes is particularly sensitive to the balance between the flexibility and the rigidity of the ligand backbone. If the degree of freedom expressed by the effective concentration[4] is sufficiently high, the monometallic complexes are obtained for the ratio $[Ln]_{tot}/[L]_{tot} = 1$. This is illustrated with symmetrical tripodal ligands, where neutral or negatively charged binding strands are attached on nitrogen[5−7] and

*To whom correspondence should be addressed. E-mail: josef.hamacek@unige.ch.

(1) (a) Mathis, G. In *Rare Earths*; Saez-Puche, R., Caro, P., Eds.; Editorial Complutense S.A.: Madrid, 1998; pp 285−298. (b) Matsumoto, K.; Yuan, J. G. Lanthanide Chelates as Fluorescent Labels for Diagnostics and Biotechnology. In *Metal Ions in Biological Systems*; Sigel, A., Sigel, H., Eds.; Marcel Dekker Inc.: New York, 2003; Vol. *40*, Chapter 6.

(2) (a) Caravan, P.; Ellison, J. J.; McMurry, T. J.; Lauffer, R. B. *Chem. Rev*. **1999**, *99*, 2293–2352. (b) *The Chemistry of Contrast Agents in Medical Magnetic Resonance Imaging*; Merbach, A. E., Toth, E., Eds.; John Wiley: London, 2001.

(3) (a) Bünzli, J.-C. G.; Piguet, C. *Chem. Rev*. **2002**, *102*, 1897–1928. (b) Bünzli, J.-C. G.; Piguet, C. *Chem. Soc. Rev*. **2005**, *34*, 1048–1077.

(4) (a) Dalla-Favera, N.; Hamacek, J.; Borkovec, M.; Jeannerat, D.; Gumy, F.; Bünzli, J.-C. G.; Ercolani, G.; Piguet, C. *Chem.—Eur. J*. **2008**, *14*, 2994–3005. (b) Canard, G.; Koeller, S.; Bernardinelli, G.; Piguet, C. *J. Am. Chem. Soc*. **2008**, *130*(3), 1025–1040.

(5) (a) Renaud, F.; Piguet, C.; Bernardinelli, G.; Bünzli, J.-C. G.; Hopfgartner, G. *J. Am. Chem. Soc*. **1999**, *121*, 9326–9342. (b) Renaud, F.; Decurnex, C.; Piguet, C.; Hopfgartner, G. *J. Chem. Soc., Dalton Trans*. **2001**, 1863–1871.

(6) (a) Imbert, D.; Comby, S.; Chauvin, A.-S.; Bünzli, J.-C. G. *Chem. Commun*. **2005**, 1432–1434. (b) Comby, S.; Imbert, D.; Vandevyver, C.; Bünzli, J.-C. G. *Chem.—Eur. J*. **2007**, *13*, 936–944. (c) Bretonnière, Y.; Wietzke, R.; Lebrun, C.; Mazzanti, M.; Pécaut, J. *Inorg. Chem*. **2000**, *39*, 3499–3505. (d) Charbonnière, L. J.; Weibel, N.; Retailleau, P.; Ziessel, R. *Chem.—Eur. J*. **2007**, *13*(1), 346–358.

(7) Senegas, J.-M.; Bernardinelli, G.; Imbert, D.; Bünzli, J.-C. G.; Morgantini, P.-Y.; Weber, J.; Piguet, C. *Inorg. Chem*. **2003**, *42*, 4680–4695.

 Published on Web 12/18/2009

carbon anchor,[8] or alternatively on triazacyclononane,[9] and wrapped about a Ln(III) cation in a helical fashion. However, introducing some constraints into the C_3-symmetrical ligands, that is, by shortening the spacer between the anchor and the binding sites, may lead to discrete polynuclear complexes, whereby each ligand strand is coordinated to another cation.[10,11]

In spite of the use of nine-coordinated complexes in luminescent probes, the analytical interest of tripodal ligands and related lanthanide complexes is rather based on exploring unsaturated complexes (i) in contrast agents (relaxivity of water molecules), or (ii) in anionic sensors as alternatives to the DOTA-based compounds.[12] In these systems, efficient sensitization of Ln(III) luminescence is achieved by using pyridine-based coordination strands,[13] usually negatively charged because of the presence of terminal carboxylates. Appropriate tripodal receptors are thus derived from C_3-symmetrical nine-coordinating ligands by removing one or more coordinating atoms. In these cases, the positions in the coordination polyhedron unoccupied by the ligand may be used for interacting with solvent molecules (i.e., water) or anions; both actions will change the solvent relaxivity in Gd(III) compounds or luminescence of a Ln(III) cation. In other words, the emission intensity is modulated by the interaction of anionic analytes or water with the first coordination sphere of Ln(III). Several highly luminescent Ln(III) complexes with hepta- or octadentate tripodal unsymmetrical ligands containing non-equivalent binding sites were successfully used for labeling purposes[14] or anionic sensing.[15] An important family of tripodal C_3-symmetrical ligands is derived from hydroxypyridonate tripodal ligands.

Scheme 1. Synthesis of **L**

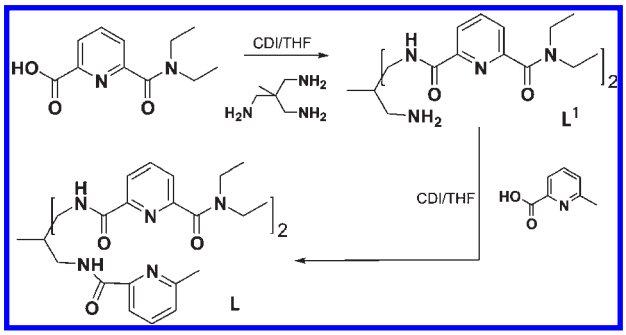

Despite the only hexacoordinate cavity provided by the ligand, these complexes show good stability, relaxivity, and efficient luminescence sensitization.[16] The attachment of two carboxypyridine and one carboxylate or phosphonate binding strands on triazacyclononane platform yields octadentate ligands, which also form Ln(III) complexes with promising properties.[17]

In this work we report on the synthesis of a new unsymmetrical tripodal ligand **L** providing potentially eight coordinating atoms on three strands attached to the carbon anchor with a short spacer. Its coordination properties with Ln(III) were studied in view of potential applications in sensing and relaxivity agents. The resulting complexes with lanthanides have been examined with different methods (NMR, ESMS, spectrophotometry) to elucidate their structure, stability, and photophysical properties in the solid state and in solution. We discuss the impact of the ligand design on the structure and properties of lanthanide complexes.

Results and Discussion

Ligand Synthesis, Structure, and Properties. The ligand **L** was prepared by a multistep synthesis according to Scheme 1. We first coupled 6-(*N*,*N*-diethylcarbamoyl)-pyridine-2-carboxylic acid[13] with 1,1,1-tris(aminomethyl)ethane (TAME) under stoichiometric conditions 2:1 and, using CDI reagent, we obtained the bifunctionalized intermediate $\mathbf{L^1}$, which was then converted to the final ligand **L** by the reaction with the bidentate synthon 2-methyl-6-carboxypyridine prepared by the oxidation of 2,6-lutidine according to the procedure described previously.[18]

The room temperature ^{1}H NMR spectrum of **L** in acetonitrile (Figure 1) shows 16 signals, a result that is compatible with the presence of the mirror plane providing the identical chemical shifts for two equivalent tridentate strands. Moreover, this fact is supported by two times higher peak areas for the aromatic protons H4−H6 in comparison with the protons H13−H15 on the short bidentate strand. All protons were completely assigned using 2D NMR spectroscopy techniques (COSY). Although we could expect a mixture of several isomers resulting from the blocked rotation about OC−N bonds in secondary amides (the *E* and *Z* notations), the presence of single signals for protons H2 and H11 indicates (i) fast interconversions on the NMR time scale of these optical

(8) (a) Koeller, S.; Bernardinelli, G.; Piguet, C. *Dalton Trans.* **2003**, 2395–2404. (b) Koeller, S.; Bernardinelli, G.; Bocquet, B.; Piguet, C. *Chem.—Eur. J.* **2003**, *9*, 1062–1074.

(9) (a) Tei, L.; Baum, G.; Blake, A. J.; Fenske, D.; Schröder, M. *J. Chem. Soc., Dalton Trans.* **2000**, 2793–2799. (b) Charbonnière, L. J.; Ziessel, R.; Guardigli, M.; Roda, A.; Sabbatini, N.; Cesario, M. *J. Am. Chem. Soc.* **2001**, *123*, 2436–2437. (c) Ziessel, R.; Charbonnière, L. J. *J. Alloys Compd.* **2004**, *374*, 283–288. (d) Gateau, C.; Mazzanti, M.; Pecaut, J.; Dunand, F. A.; Helm, L. *Dalton Trans.* **2003**, 2428–2433. (e) Giraud, M.; Andreiadis, E. S.; Fisyuk, A. S.; Demadrille, R.; Pecaut, J.; Imbert, D.; Mazzanti, M. *Inorg. Chem.* **2008**, *47*(10), 3952–3954. (f) Nonat, A.; Imbert, D.; Pecaut, J.; Giraud, M.; Mazzanti, M. *Inorg. Chem.* **2009**, *48*(9), 4207–4218.

(10) Bretonnière, Y.; Mazzanti, M.; Wietzke, R.; Pécaut, J. *Chem. Commun.* **2000**, 1543–1544.

(11) Hamacek, J.; Bernardinelli, G.; Filinchuk, Y. *Eur. J. Inorg. Chem.* **2008**, *22*, 3419–3422.

(12) (a) Parker, D.; Dickins, R. S.; Puschmann, H.; Crossland, C.; Howard, J. A. K. *Chem. Rev.* **2002**, *102*, 1977–2010. (b) Parker, D. *Coord. Chem. Rev.* **2000**, *205*, 109–130. (c) Parker, D.; Yu, J. *Chem. Commun.* **2005**, 3141–3143. (d) Dickins, R. S.; Gunnlaugsson, T.; Parker, D.; Peacock, R. D. *Chem. Commun.* **1998**, 1643–1644.

(13) (a) Piguet, C.; Bünzli, J.-C. G.; Bernardinelli, G.; Hopfgartner, G.; Petoud, S.; Schaad, O. *J. Am. Chem. Soc.* **1996**, *118*, 6681–6697. (b) Chatterton, N.; Bretonniere, Y.; Pecaut, J.; Mazzanti, M. *Angew. Chem., Int. Ed.* **2005**, *44*, 7595–7598.

(14) (a) Weibel, N.; Charbonnière, L. J.; Guardigli, M.; Roda, A.; Ziessel, R. F. *J. Am. Chem. Soc.* **2004**, *26*, 4888–4896. (b) Charbonnière, L.; Mameri, S.; Kadjane, P.; Platas-Iglesias, C.; Ziessel, R. *Inorg. Chem.* **2008**, *47*, 3748–3762. (c) Charbonnière, L. J.; Mameri, S.; Flot, D.; Waltz, F.; Zandanel, C.; Ziessel, R. F. *Dalton Trans.* **2007**, 2245–2253.

(15) (a) Mameri, S.; Charbonnière, L. J.; Ziessel, R. *Inorg. Chem.* **2004**, *43*, 1819–1821. (b) Charbonnière, L. J.; Ziessel, R.; Montalti, M.; Prodi, L.; Zaccheroni, N.; Boehme, C.; Wipff, G. *J. Am. Chem. Soc.* **2002**, *124*, 7779–7788.

(16) (a) Jocher, C. J.; Moore, E. G.; Xu, J.; Avedano, S.; Botta, M.; Aime, S.; Raymond, K. N. *Inorg. Chem.* **2007**, *46*, 9182–9191. (b) Seitz, M.; Pluth, M. D.; Raymond, K. N. *Inorg. Chem.* **2007**, *46*, 351–353. (c) Moore, E. G.; Xu, J.; Jocher, C. J.; Castro-Rodriguez, I.; Raymond, K. N. *Inorg. Chem.* **2008**, *47*, 3105–3118.

(17) (a) Nonat, A.; Gateau, C.; Fries, P. H.; Mazzanti, M. *Chem.—Eur. J.* **2006**, *12*(27), 7133–7150. (b) Nonat, A.; Giraud, M.; Gateau, C.; Fries, P. H.; Helm, L.; Mazzanti, M. *Dalton Trans.* **2009**, 8033–8046.

(18) Black, G.; Depp, E.; Corson, B. B. *J. Org. Chem.* **1949**, *14*, 14–21.

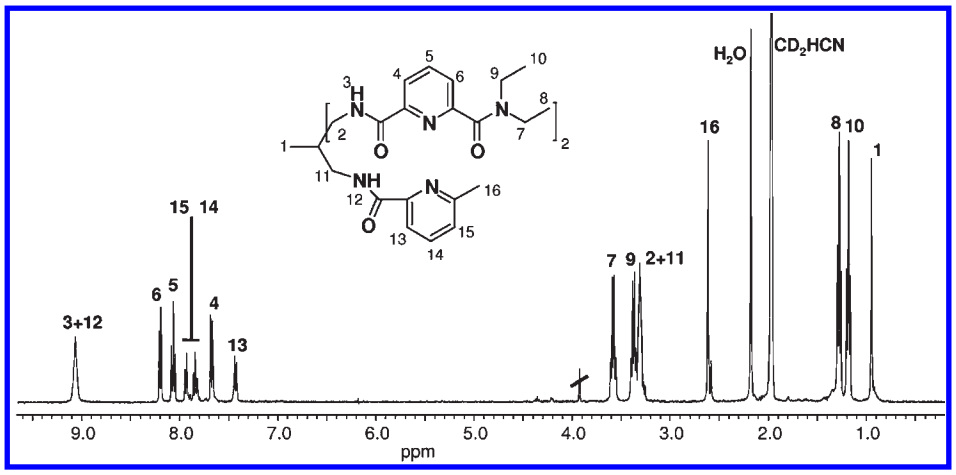

Figure 1. ^{1}H NMR of **L** with atom numbering (293 K, CD_3CN).

Scheme 2. Possible Conformations of the Bidentate Strand in the Free Ligand **L**

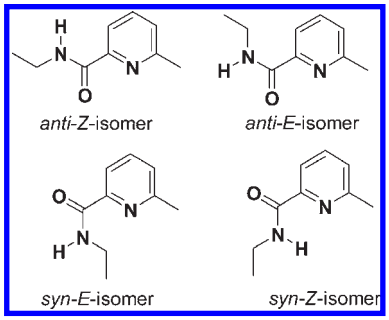

isomers and therefore a low free energy difference for this process, or (ii) the stabilization of *Z* isomers for each ligand strand because of intramolecular NH···N(pyridine) hydrogen bonds producing five-membered rings in *syn-Z* conformation (Scheme 2).[19] The presence of the *syn* conformation is evidenced by the fact that no spatial coupling of pyridine protons with methylene or amide protons was observed with NOEDIF experiments.

A slow evaporation of the acetonitrile solution of **L** provided fragile crystals suitable for X-ray crystallography. Despite a lower quality of the diffraction data, we were able to access the structural parameters within this tripodal ligand. The crystal structure (Supporting Information, Figure S1) indeed showed *Z* conformations of secondary amides. In addition, a *syn* conformation was adopted to minimize the repulsion between dipole moments of the central pyridine ring and the connected coplanar carbonyl group. The tertiary amides were found in a *syn* conformation with significant distortions with respect to the pyridine plane. The crystal packing was characterized by the H-bond network comprising intramolecular NH···N(pyridine) and NH···O bonds and intermolecular interactions NH···O (Supporting Information, Table S1). Finally, the solid state structure showed the exclusive formation of the *syn-syn-ZZZ* isomer in agreement with the NMR observations.

Synthesis of Lanthanide Complexes. The Ln(III) complexes (Ln = La, Eu, and Lu) were obtained by mixing perchlorate salts with **L** in stoichiometric quantities in acetonitrile. The resulting solution was thoroughly stirred and evaporated to dryness. The diffusion of *tert*-butylmethylether into the concentrated methanol solution provided fragile microcrystals that disintegrated into a microcrystalline powder when filtrated from the mother liquor. The elemental analysis of the Eu(III) complex corresponds to the molecular formula $[Eu_2L_2](ClO_4)_6\cdot 1CH_3OH\cdot 12H_2O$ (**1**). The NMR spectrum of **1** dissolved in CD_3CN is reminiscent to that obtained by direct mixing of Eu(III) perchlorate with **L** in stoichiometric conditions (Supporting Information, Figure S2).

In addition to the latter complex, the formation of complexes with the stoichiometry Ln/**L** = 2:3 was evidenced by NMR, ESMS and spectrophotometry. The solid samples of these complexes (Ln = Eu, Lu) were prepared using appropriate quantities and the procedure described above. However, numerous attempts to obtain the X-ray quality crystals of these compounds were not successful.

X-ray Crystal Structure of $[Eu_2(C_{34}H_{44}N_8O_5)_2(CH_3OH)_6](ClO_4)_6\cdot 5CH_3OH$. The recrystallization of **1** by a slow diffusion of *tert*-butylmethylether into the methanol solution provides transparent crystals suitable for the X-ray analysis, which reveals the formation of a dinuclear complex with the composition $[Eu_2(C_{34}H_{44}N_8O_5)_2(CH_3OH)_6](ClO_4)_6\cdot 5CH_3OH$. Each Eu(III) is coordinated by two tridentate dicarbonylpyridine binding strands belonging to two ligand molecules, as shown in Figure 2. Regarding the coordination environment, each Eu(III) is nine-coordinated by two pyridine nitrogens, four carbonyl groups, and three solvent molecules, that is, methanol. The coordination sphere can be described as a tricapped trigonal prism. The short strand of **L** containing methylpyridine is not coordinated to europium cations, but strongly contributes to the intermolecular stacking interactions (Supporting Information, Figure S3). The uncoordinated methylpyridine of the ligand *b* (N2b, C5b−C9b) is not ordered and is refined with restrictions and the population parameters 0.6 and 0.4. In addition to coordinated methanol molecules, the crystal structure contains five uncoordinated methanol molecules per complex.

The tridentate sites of both coordinating ligands appear to be wrapped about the axis going through both

(19) Le Borgne, T.; Bénech, J.-M.; Floquet, S.; Bernardinelli, G.; Aliprandini, C.; Bettens, P.; Piguet, C. *Dalton Trans.* **2003**, 3856–3868.

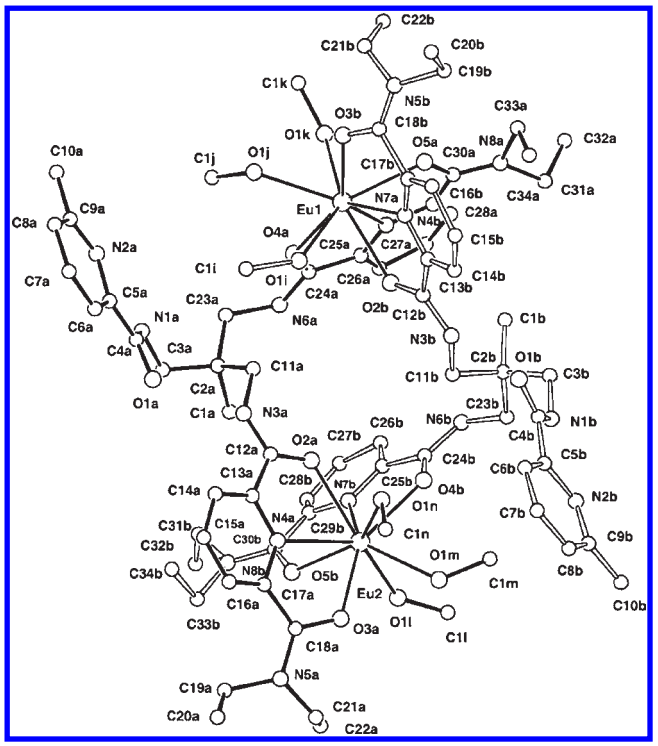

Figure 2. 3D view "ORTEP" and the atom numbering scheme of the dinuclear complex $[Eu_2\mathbf{L}_2(CH_3OH)_6]^{6+}$. Hydrogen atoms, anions, and uncoordinated solvent molecules were removed for clarity.

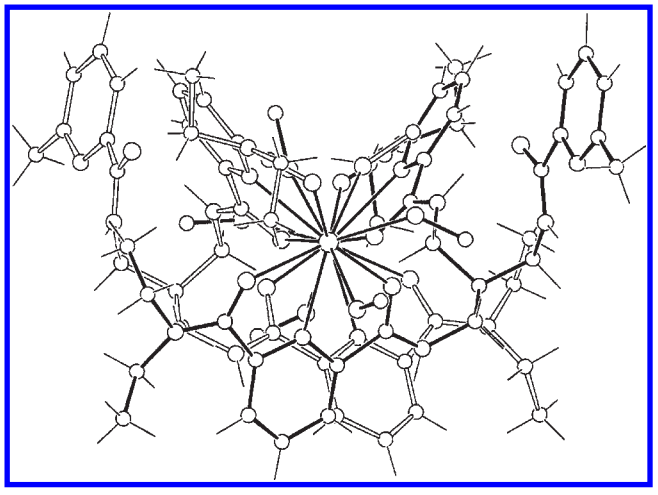

Figure 3. Side view of $[Eu_2\mathbf{L}_2(CH_3OH)_6]^{6+}$. Hydrogen atoms, anions, and uncoordinated solvent molecules were removed for clarity.

cations (Figure 3). However, the Eu(III) cations are related by the 2-fold axis (C_2) perpendicular to the latter one. The Flack parameter x is found to be 0.13(2), and this chiral crystal structure is composed of two isomers in the ratio 87(2)/13(2)%, where the major complex shows the helicity *M*. The Supporting Information, Table S2 presents selected bond lengths and angles. The average bond lengths Eu−O(carbonyl) and Eu−N in $[Eu_2\mathbf{L}_2(CH_3OH)_6]^{6+}$ are 2.40(4) and 2.58(2) Å (Supporting Information, Table S3), respectively, distances identical to those in monometallic complexes with monotopic ligand $\mathbf{L}^{\mathbf{A}}$ (Scheme 3) possessing the same coordination atoms.[20] The average bond length Eu−O(methanol) equals 2.44(1) Å, which is comparable with usual Eu−O(water) bonds.

Scheme 3. Chemical Structures of $\mathbf{L}^{\mathbf{A}}$ and $\mathbf{L}^{\mathbf{B}}$

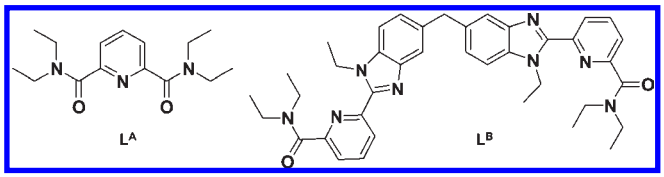

The structure of $[Eu_2\mathbf{L}_2(CH_3OH)_6]^{6+}$ can be compared with the unsaturated dinuclear complex previously formed with $\mathbf{L}^{\mathbf{B}}$, which possesses a rigid biphenyl spacer (Scheme 3). In $[Eu_2\mathbf{L}^{\mathbf{B}}_2]^{6+}$, two triflate anions and one water molecule complete the coordination sphere.[21] The latter complex adopts an achiral side-by-side arrangement, while the $[Eu_2\mathbf{L}_2(CH_3OH)_6]^{6+}$ cation is chiral and forms a "pseudo cavity" between metallic cations separated by 8.87(1) Å . Using a flexible aliphatic spacer in **L** leads to the same intermetallic distances as in $[Eu_2\mathbf{L}^{\mathbf{B}}_2]^{6+}$ (9.05(3) Å).[21]

NMR Investigations and Solution Properties of Ln(III) Complexes with L. To establish the complete speciation of Ln(III) complexes in acetonitrile, ^{1}H NMR titrations of **L** were performed with the diamagnetic cations (Ln = La and Lu) allowing a better identification of signals. The [Ln]/[**L**] ratio was varied from 0 to 2 ([**L**] $\sim 2 \times 10^{-2}$ M), and each spectrum was taken at least 1 h after the addition of Ln(III) solution to achieve re-equilibrating of the mixture.

A careful analysis of the obtained ^{1}H NMR spectra shows that the signals belonging to the free **L** are detected until the ratio [Ln]/[**L**] about 0.5 for both titrations (Figure 4, Supporting Information, Figures S4 and S5). Interestingly, the signals for the bidentate strand (i.e., H16) show only minor chemical shifts and some broadening comparing to the signals of free **L**. This observation is compatible with the fact that the bidentate unit is not coordinated to metallic cations. Some discrepancies between these titrations are discussed below.

In case of Lu(III) titration (Figure 4 and Supporting Information, Figure S4), the formation of at least four major species is evidenced with the help of a qualitative distribution diagram (Supporting Information, Figure S6), which is constructed by plotting the relative areas of selected well-resolved peaks versus metal/ligand ratio. The maxima of the peak area are estimated for the molar ratios [Lu]/[**L**] about 0.3, 0.65, and 1; these represent the formation of complexes $[Lu\mathbf{L}_3]^{3+}$, $[Lu_2\mathbf{L}_3]^{6+}$, and $[Lu_2\mathbf{L}_2]^{6+}$. The last species, probably $[Lu_2\mathbf{L}]^{6+}$ or $[Lu_3\mathbf{L}]^{9+}$, is formed in excess of metal ([Lu]/[**L**] > 1). While the spectra are relatively well-resolved until [Lu]/[**L**] = 0.9, the peaks become larger for higher ratios, and it prevents further interpretation in terms of the structure. This can be attributed (i) to a slow ligand exchange within these unsaturated complexes, (ii) to a slow interconversion on the NMR time scale between the enantiomeric forms of

(20) Renaud, F.; Piguet, C.; Bernardinelli, G.; Bünzli, J.-C. G.; Hopfgartner, G. *Chem.—Eur. J.* **1997**, *3*, 1646–1659.

(21) Martin, N.; Bünzli, J.-C. G.; McKee, V.; Piguet, C.; Hopfgartner, G. *Inorg. Chem.* **1998**, *37*, 577–589.

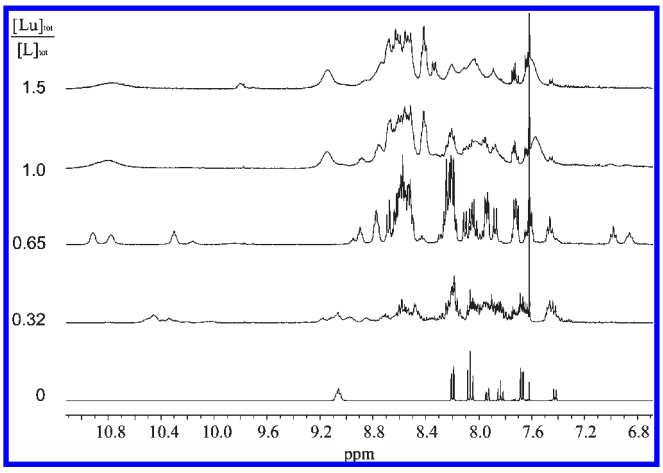

Figure 4. Part of the selected ^{1}H NMR spectra showing the signals of aromatic and amide protons for the titration of **L** with Lu(III). [**L**] = 2.5×10^{-2} M.

$[Ln_2\mathbf{L}_2]^{6+}$, and (iii) to a certain structural disorder of the binding strands also translated in increased uncertainties during the refinement of crystallographic data. In spite of these difficulties, we have attempted to assign, at least qualitatively, the ^{1}H NMR signals of Lu(III) complexes with the help of the 2D NMR spectroscopy technique (COSY). For the spectrum with [Lu]/[**L**] = 1 (Supporting Information, Figure S7), we could recognize seven pyridine entities (H5, H14) and seven signals corresponding to amidic protons (H3, H12), which is more than expected from the crystal structure. However, $[Lu_2\mathbf{L}_3]^{6+}$ is still present in solution at this stoichiometric ratio (Supporting Information, Figure S6) and the contribution of these protons appears in the spectrum. Nevertheless, the observed signals indicate the presence of several non-equivalent ligand strands, which is tentatively attributed to different conformations of unsaturated $[Ln_2\mathbf{L}_2]^{6+}$ complexes. The measurements at variable temperature do not result in significant simplifications of the spectrum up to 70 °C, except additional broadening (Supporting Information, Figure S8).

For the spectrum with [Lu]/[**L**] = 0.65 (Supporting Information, Figure S7), at least 6 different pyridine (H5, H14) and 10 amide protons (H3, H12) were assigned in the spectrum. The observation of multiplets for diastereotopic methylene protons indicates a helical wrapping of strands in the complex. Three singlet peaks between 0.1 and 0.7 ppm, attributed to methyl protons of the anchor, show the presence of three different ligands, which excludes the formation of classical triple-stranded dinuclear helicates. However, a more precise information on the structure of the $[Lu_2\mathbf{L}_3]^{6+}$ species could not be extracted.

The ^{1}H NMR spectra of isolated complexes $[Lu_2\mathbf{L}_3]^{6+}$ and $[Lu_2\mathbf{L}_2]^{6+}$ are closely related to those obtained by direct mixing in solution (Supporting Information, Figure S9) and do not provide more information about their structure. Larger less-resolved peaks may be attributed to thermodynamic re-equilibrating after dissolution of solid compounds and to dynamic processes occurring in solution.

In case of the titration with La(III), the evolution of ^{1}H NMR signals (Supporting Information, Figure S5) significantly differs from that observed in the titration with Lu(III). The first complex species appears for the molar ratio about [La]/[**L**] = 0.5 and is stepwise transformed to another complex. The spectrum does not significantly change from [La]/[**L**] = 0.8−0.9 and that points to the presence of $[La_2\mathbf{L}_3]^{6+}$ species. In excess of metal, the overall spectrum remains almost unchanged except for a new peak at 9.45, tentatively attributed to an amide proton. Relatively simple NMR spectra of all La(III) complexes indicate the presence of a symmetry element.

It may be concluded that the above-described NMR experiments well established the stoichiometry of complex species along the titrations. However, the collected spectra do not allow to explicitly deduce their structure in solution.

ESMS Titrations. The recording of reliable ESMS spectra of Ln(III) complexes with **L** requires the optimization of ionization conditions to achieve sufficient ionization of complexes, as well as to prevent their dissociation. In our case, the ESMS spectra of acetonitrile solutions were thus measured at 150 °C. The identification of complex species forming the series of perchlorate adducts was confirmed by comparing measured and calculated isotopic profiles.

ESMS titrations were performed for mixtures of $Ln(ClO_4)_3 \cdot xH_2O$ (Ln = La, Eu, Lu) and **L** ([**L**] = 3×10^{-4} M) with the [Ln]/[**L**] ratio 0−4 in acetonitrile. Along the titration, a successive formation of species with several stoichiometries was evidenced for all metals. In excess of ligand ([Ln]/[**L**] ≤ 0.5), major species with stoichiometries $Ln\mathbf{L}_2$ and $Ln\mathbf{L}_3$ were observed, as well as the free ligand **L**. When the Ln(III) concentration is increased to [Ln]/[**L**] = 0.67, new signals appear and the spectra are dominated by $Ln_2\mathbf{L}_3$ complexes and their perchlorate adducts (Figure 5a). The situation becomes slightly different at [Ln]/[**L**] = 1 (Figure 5b and Supporting Information, Figure S10). The complexes $Ln_2\mathbf{L}_3$ are highly present, but the $Ln_2\mathbf{L}_2$ complexes turn into the major species. In excess of metal, the later complexes still dominate the spectra, while only traces of $Ln_2\mathbf{L}$ are detected because of possible difficulties to transfer such solvated species into the gaseous phase (Figure 5c).[21,22] The speciation measured with ESMS thus shows the same trend as the data provided by NMR titrations. The ESMS spectra of in situ mixtures are reminiscent to those recorded for isolated solid compounds (i.e., with Eu(III), Supporting Information, Figure S11) except a lower intensity detected for the $[Eu_2\mathbf{L}_2]^{6+}$ complex.

Solution Properties of $[Ln_2\mathbf{L}_2(ClO_4)_6]$. The spectrophotometric batch titration of **L** ($\sim 3 \times 10^{-4}$ M) with $Ln(ClO_4)_3 \cdot xH_2O$ (Ln = La, Nd, Eu, Tb, Er, Lu) were performed in acetonitrile for the ratio $[Ln]_{tot}/[\mathbf{L}]_{tot}$ = 0−5. The solutions were allowed to equilibrate for 48 h and measured at 25.0 ± 0.1 °C in quartz cuvettes (l = 0.1 cm).

The variations of the absorption spectra (Figure 6) were adjusted with the SPECFIT program. The factor analysis indicates the presence of several absorbing complex species, and the best thermodynamic model comprises the species previously observed during ESI-MS. Contrary to the NMR titrations, the measured spectrophotometric

(22) (a) Piguet, C.; Rivara-Minten, E.; Hopfgartner, G.; Bünzli, J.-C. G. *Helv. Chim. Acta* **1995**, *78*, 1541–1566. (b) Piguet, C.; Bünzli, J.-C. G.; Bernardinelli, G.; Hopfgartner, G.; Petoud, S.; Schaad, O. *J. Am. Chem. Soc.* **1996**, *118*, 6681–6697.

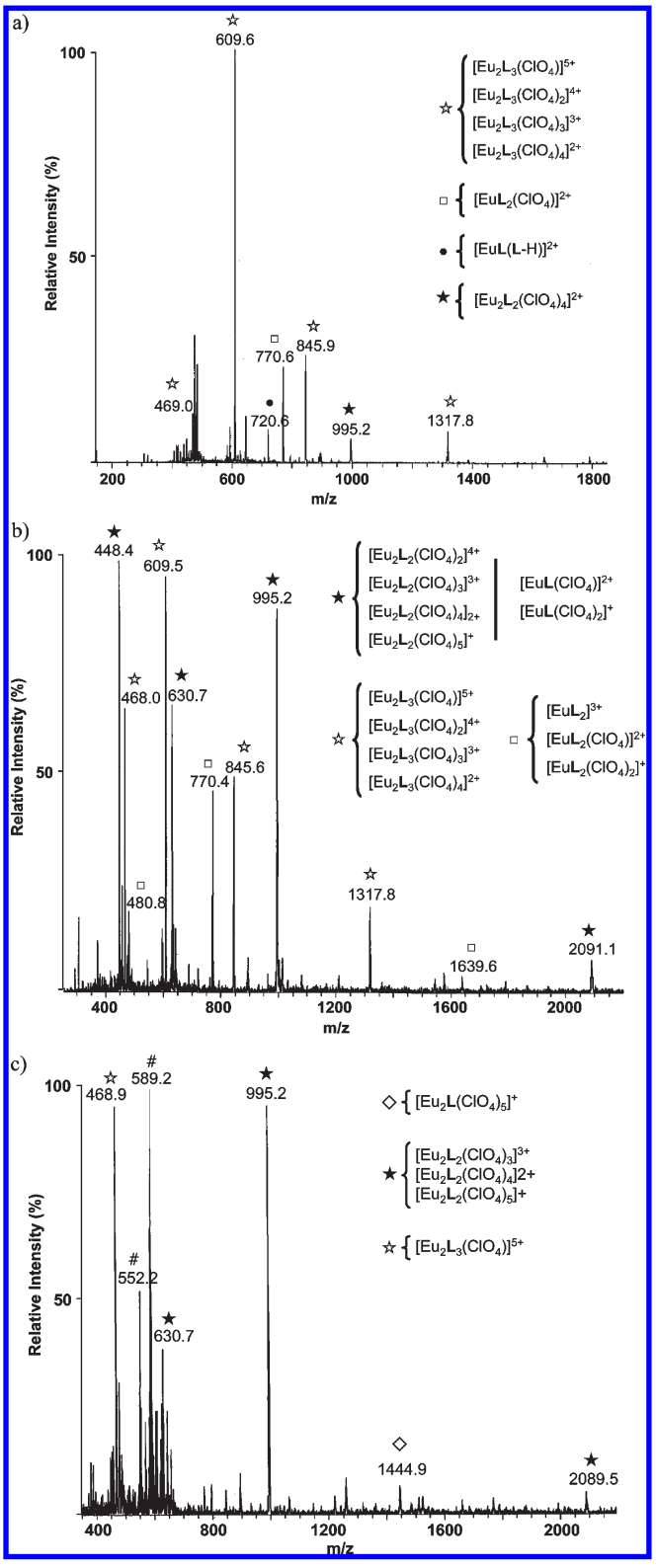

Figure 5. ESMS titration of **L** with Eu(III) in acetonitrile. Spectrum for (a) [Eu]/[**L**] = 0.67; (b) [Eu]/[**L**] = 1; and (c) [Eu]/[**L**] = 4 (# corresponds to Eu(III) clusters appearing in excess of metal).

data fit better with the complexes $[LnL_2]^{3+}$. The related macroscopic formation constants are associated with the following equilibria (eqs 1−4):

$$Ln(III) + 2L \rightleftarrows [LnL_2]^{3+} \qquad \beta_{12} \qquad (1)$$

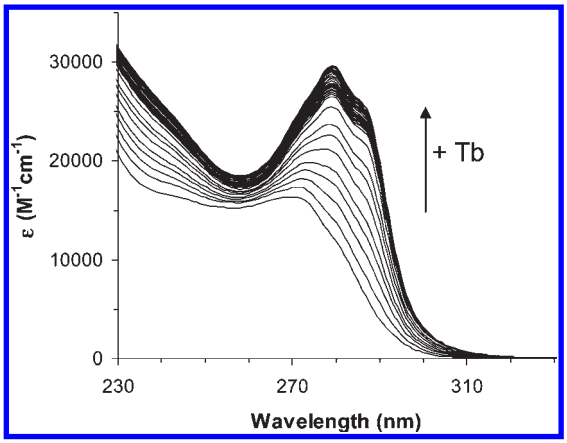

Figure 6. Variation of the absorption spectra for the spectrophotometric batch titration of **L** with $Tb(ClO_4)_3$.

$$2Ln(III) + 3L \rightleftarrows [Ln_2L_3]^{6+} \qquad \beta_{23} \qquad (2)$$

$$2Ln(III) + 2L \rightleftarrows [Ln_2L_2]^{6+} \qquad \beta_{22} \qquad (3)$$

$$2Ln(III) + L \rightleftarrows [Ln_2L]^{6+} \qquad \beta_{21} \qquad (4)$$

The fitted values of log β_{mn} for titrations with six selected Ln(III) are summarized in Table 1. All titrations exhibit a clear inflection point about the [Ln]/[**L**] = 0.67, which indicates the formation of species $[Ln_2L_3]^{6+}$. For La(III) and Nd(III), the absorption changes in excess of ligand can be fitted by considering $[LnL_2]^{3+}$. However, its concentration is apparently lower for remaining lanthanide complexes (Ln = Eu−Lu), which does not allow reliable determination of the stability constant. Nevertheless, log β_{12} is estimated to be about 13 using the data at the beginning of the titrations. The absorption changes are much less pronounced for [Ln]/[**L**] > 0.67, where the constants for $[Ln_2L_2]^{6+}$ could be fitted only for titrations with Eu−Lu. In excess of metal, slight spectral variations are best fitted with the species $[Ln_2L]^{6+}$, already detected by ESMS. The stability constants for $[Ln_2L_2]^{6+}$, $[Ln_2L_3]^{6+}$, and $[Ln_2L]^{6+}$ are almost invariable along the series, within experimental errors (Figure 7). It appears, that for bigger cations (i.e., La(III)) the assembly process favors the $[Ln_2L_3]^{6+}$ complexes that undergo the transformation in excess of smaller lanthanides (i.e., Lu(III)) to provide $[Ln_2L_2]^{6+}$ and $[Ln_2L]^{6+}$ complexes. The distribution curves calculated with the fitted stability constants for heavier lanthanides (e.g., Tb(III), Supporting Information, Figure S12a) are in qualitative agreement with the speciation observed within the NMR titration (Supporting Information, Figure S6). As illustrated for the spectrophotometric titration with Tb(III) in Figure 6, the fitted spectra of different species are correlated (Supporting Information, Figure S12b), which contributes to the relatively big errors estimated during the fitting process.

The stability constants of $[Ln_2L_2]^{6+}$ and $[Ln_2L_3]^{6+}$ are lower, but still comparable with those obtained for

Table 1. Stability Constants for the Ln(III) Complexes with **L** (Acetonitrile, 298 K)[a]

Ln(III)	$1/r$ [Å^{-1}] [b]	log β_{12}	log β_{23}	log β_{22}	log β_{21}
La	0.8197	14.3 ± 0.9	25.5 ± 1.0		
Nd	0.8621	14.5 ± 1.0	26.0 ± 1.2		
Eu	0.8929	~13	23.8 ± 1.2	19.2 ± 1.1	10.8 ± 0.9
Tb	0.9091	~13	23.6 ± 0.7	17.6 ± 0.7	10.9 ± 0.5
Er	0.9434	~13	24.5 ± 0.9	17.9 ± 0.8	11.3 ± 0.6
Lu	0.9709	~13	24.5 ± 0.6	19.1 ± 0.5	11.7 ± 0.7

[a] Fitted according to the equilibria eqs 1−4. [b] Ionic radii for nine-coordinate Ln(III).

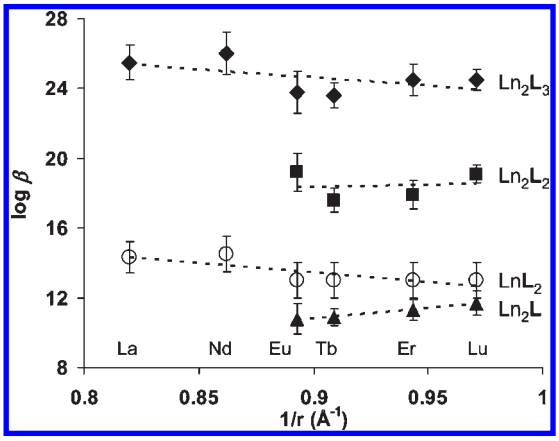

Figure 7. Plot of the fitted stability constants of Ln_mL_n complexes versus inverse ionic radius. The trendlines are only guides for the eyes.

the ligand $\mathbf{L}^{\mathbf{B}}$.[23] This probably results from the similar structure of these dinuclear complexes, whereby almost identical intermetallic distances Eu−Eu induce comparable electrostatic repulsions. On the other hand, the presence of a flexible spacer in **L** can be responsible for a slight decrease of the overall stability.

Photophysical Properties of $[Eu_2L_2](ClO_4)_6$ in the Solid State. According to the elemental analysis of the isolated complex **1**, water molecules are coordinated to the Eu(III) cations instead of methanol found in the crystal structure. This compound was thus investigated by spectroscopic methods to confirm its dinuclear structure. The excitation spectra were measured for different λ_{an} at 10 K and show the same profiles except for the intensity (Supporting Information, Figure S13).

The high resolution emission spectrum recorded at 10 K (Figure 8) shows the bands $^5D_0 \rightarrow {}^7F_j$ (j = 0−6) typical for Eu(III) complexes. The spectra remain almost unchanged with increasing temperature except for broadening. Thorough examination of the f → f transitions at 10 K shows the presence of 3 peaks for $^5D_0 \rightarrow {}^7F_1$ transitions, 5 levels for $^5D_0 \rightarrow {}^7F_2$ transitions, and the splitting of transitions $^5D_0 \rightarrow {}^7F_4$ into 9 bands (Supporting Information, Table S3, Figure S14). This overall splitting pattern is typical for the coordination site of a low symmetry and is compatible with C_1, C_2, or C_s symmetry groups. This result is in a qualitative agreement with the crystal structure of $[Eu_2L_2]^{6+}$. The high resolution excitation and emission spectra at 10 K reveal the presence of only one peak for the transitions $^5D_0 \leftarrow {}^7F_0$ and $^5D_0 \rightarrow {}^7F_0$

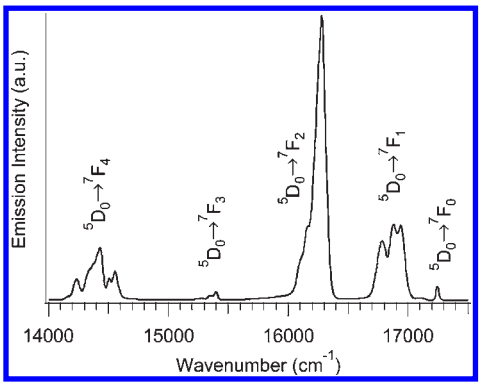

Figure 8. Emission spectrum of **1** at 10 K (high resolution, excitation at 270 nm).

sensitive to the chemical environment of the Eu(III) cation. This implies the existence of a single crystallographic site for the metallic cation.[24] Moreover, its intensity, quite small compared with other transitions, reflects a small population of this state forbidden by the symmetry selection rules. This is in agreement with the C_2 symmetry of the crystallographic site shown previously by the crystal structure of $[Eu_2L_2]^{6+}$, where both Eu(III) cations are equivalent.

It is known that the composition of the Eu(III) coordination sphere influences the total charge through the nephelauxetic effect modifying the energy of the $^5D_0 \leftarrow {}^7F_0$ transition. This deviation can be calculated according to the Frey and Horrocks equation (eq 5),[25] whereby $\tilde{\nu}_0$ is 17374.0 cm^{-1}, the free metal ion value, C_{CN}, accounts for 1 for the nine-coordinated Eu(III) cation, n_i is the number of type i, and δ_i is the capacity of the atom i to accept the electronic density of the metal ion. The coordination sphere of each metal ion in **1** is considered as that of the crystal structure: two heterocyclic nitrogens (δ_i = −15.3 cm^{-1}),[22] four oxygen atoms coming from carboxamide groups (δ_i = −15.7 cm^{-1}), and three oxygen atoms of water molecules (δ_i = −10.4 cm^{-1}).

$$\tilde{\nu} = \tilde{\nu}_0 + C_{CN} \cdot \sum n_i \delta_i \qquad (5)$$

The straightforward calculation gives the value $\tilde{\nu}$ = 17249.4 cm^{-1}. Measuring of the energy of Eu($^5D_0 \leftarrow {}^7F_0$) at 295 K gives $\tilde{\nu}_{exp}$ = 17257 cm^{-1}, which is close to $\tilde{\nu}_{exp}$ = 17255.9 cm^{-1} recalculated from measurements at 10 K ($\tilde{\nu}_{exp}$ = 17244.1 cm^{-1}) by taking into account the semi-empirical temperature correction 1 cm^{-1}/24 K.[23] We deduce that the calculated value lies relatively close to the measured one ($\Delta\tilde{\nu}$ = 7.6 cm^{-1}). Although such differences are generally accepted in literature,[5,26] this effect can be tentatively explained by diminishing the nephelauxetic parameters of coordinating atoms,[21] very sensitive to the coordinating environment, by somewhat longer coordination bond lengths (i.e., the distance Eu−N = 2.58 (Supporting Information, Table S2) comparing

(23) Zeckert, K.; Hamacek, J.; Rivera, J.-P.; Floquet, S.; Pinto, A.; Borkovec, M.; Piguet, C. *J. Am. Chem. Soc.* **2004**, *126*, 11589–11601.

(24) Bünzli, J.-C. G. In *Lanthanide Probes in Life, Chemical and Earth Sciences*; Bünzli, J.-C. G., Choppin, G. R., Eds.; Elsevier: Amsterdam, 1989; Chapter 7.

(25) Frey, S. T.; Horrocks, W. de W. *Inorg. Chim. Acta* **1995**, *228*, 383–390.

(26) Bünzli, J.-C. G.; Charbonnière, L. J.; Ziessel, R. F. *J. Chem. Soc., Dalton Trans.* **2000**, 1917–1923.

Table 2. Values of $\tilde{\nu}$ Calculated for Three Possible Conformations Given in the Supporting Information, Figure S11

i	n_i (I)	n_i (II)	n_i (III)	n_i (IV)
N-heterocyclic[a]	1	2	2	3
O-water	6	3	4	1
O-amide carbonyl	2	4	3	5
$\tilde{\nu}$ (cm^{-1})	17266.6	17252.8	17257.5	17244.3

[a] $\delta_{\text{N-heterocyclic}} = -13.6\ cm^{-1}$ (from ref 28).

to 2.568(7) Å in tripodal complexes,[5] for instance). A recent spectroscopic analysis of benzimidazole-pyridine podates led to the reconsideration of $\delta_{\text{N-heterocyclic}}$ to provide the value $-13.6\ cm^{-1}$.[27] The subsequent application of eq 5 gives the new estimation $\tilde{\nu} = 17252.8\ cm^{-1}$, in better correlation with the experiment. For the sake of comparison, we have calculated the energy of the $^5D_0 \leftarrow {}^7F_0$ transition for different compositions of the coordination sphere related to the hypothetical Ln_mL_n ($m = n$) species modeled in Supporting Information, Figure S15. The number of coordinating atoms in each unsaturated complex was completed up to nine by water oxygens (Table 2). The parameters δ_i given above were used for calculating the expected position of the $^5D_0 \leftarrow {}^7F_0$ transition according to eq 5, and the results are summarized in Table 3. It shows that the experimental value $\tilde{\nu}$ is close to the configurations II and III with interchanged tridentate and bidentate strands, where two ligand strands are implied in the coordination. This is qualitatively confirmed by the crystal structure of the dinuclear complex $[Eu_2L_2]^{6+}$. On the contrary, the configurations I and IV can be definitely excluded.

Luminescence lifetime measurements are used to estimate effectiveness of the energy transfer of a chromophore to the lanthanide cation. A monoexponential decrease of luminescence of **1** was observed for different λ_{em}. In the solid state, the fitted values do not significantly vary with temperature (Table 3). For instance, for $\lambda_{em} = 615$ nm the lifetimes are distributed around the average value $\tau = 0.46(2)$ ms, but a slightly lower value ($\tau = 0.28(3)$ ms) is observed for $\lambda_{em} = 580$ nm at a very low emission intensity. Nevertheless, these values are compatible with the presence of three water molecules in the europium coordination sphere.[28] However, the dissolving of **1** in acetonitrile increases the lifetimes up to 1.19(2) ms, which represents a considerable improvement because of the replacement of water molecules in the first coordination sphere by acetonitrile. The low-resolution emission spectrum of **1** dissolved in acetonitrile or methanol is reminiscent to that of the solid compound (Figure 9).

The number of solvent molecules can be estimated from the well-known Sudnick and Horrocks equation, whereby τ_H and τ_D correspond to the lifetimes in normal and deuterated solvent, respectively. In our case, CH_3OH and CH_3OD were used to dissolve the complex and eq 6 is considered for calculating the number of coordination

Table 3. Lifetimes Measured for **1** as Function of Temperature and λ_{em} (nm)

	τ (ms), solid state				τ (ms), solution	
temperature [K]	λ_{em} = 580 [a]	λ_{em} = 592[a]	λ_{em} = 615 [a]	λ_{em} = 617[b]	λ_{em} = 617[b] CH_3CN	λ_{em} = 617 [b] MeOH
10	0.26	0.41	0.47			
77	0.27	0.39	0.45	0.36		
100	0.25	0.39	0.44			
150	0.25	0.39	0.42			
200	0.31	0.42	0.46			
250	0.31	0.44	0.48			
295				0.31	1.19	0.46
300	0.31	0.44	0.47			

[a] $\lambda_{ex} = 355$ nm. [b] $\lambda_{ex} = 270$ nm. Errors on the fitted lifetimes are estimated to 0.01 ms.

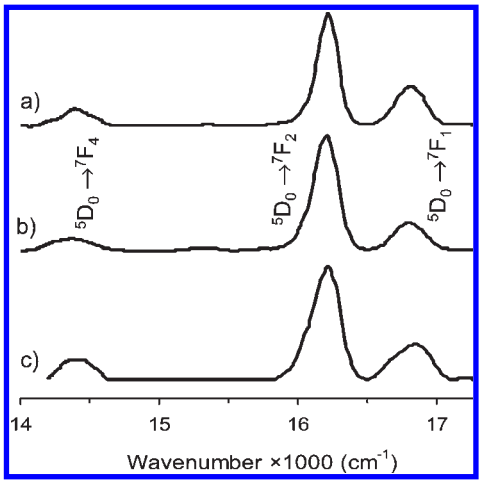

Figure 9. Low resolution emission spectra of **1** (a) at room temperature (solid state), (b) in acetonitrile, and (c) in methanol. $\lambda_{exc} = 270$ nm.

sites occupied by CH_3OH.[28−30]

$$n = 2.1\left(\frac{1}{\tau_H} - \frac{1}{\tau_D} - 0.125\right) \qquad (6)$$

The values of τ_H and τ_D for $[Eu_2L_2]^{6+}$ are found to be 0.46 and 1.74 ms. The application of eq 6 gives $n = 3.1 \pm 0.5$, which corresponds to approximately three methanol molecules per metallic binding site. This result is in good agreement with the number of solvent molecules determined by crystallography and suggests that the dinuclear structure is maintained in methanol.

Conclusions

The present work deals with a thorough investigation of lanthanide complexes with a new asymmetric tripodal ligand **L**, whose synthesis has been developed and optimized. The structure of **L** has been elucidated in solution by NMR indicating the presence of a single *syn-syn-ZZZ* isomer. In the solid state, the molecules of **L** are held together by a number of hydrogen bonds, and the structure is compatible with the NMR observations. A combination of ES-MS, NMR, spectrophotometry, and crystallography allowed to characterize Ln(III) complexes with **L**. First, the crystal

(27) Ryan, P. E.; Guénée, L.; Canard, G.; Gumy, F.; Bünzli, J.-C. G.; Piguet, C. *Inorg. Chem.* **2009**, *48*(6), 2549–2560.
(28) (a) Horrocks, W. D., Jr.; Sudnick, D. R. *J. Am. Chem. Soc.* **1979**, *101* (2), 334–340. (b) Horrocks, W. D., Jr.; Sudnick, D. R. *Acc. Chem. Res.* **1981**, *14*, 384–392.
(29) Holz, R. C.; Chang, C. A.; Horrocks, W. D., Jr. *Inorg. Chem.* **1991**, *30*, 3270–3275.
(30) Beeby, A.; Clarkson, J. M.; Dickins, R. S.; Faulkner, S.; Parker, D.; Royle, L.; de Sousa, A. S.; Williams, J. A. G.; Woods, M. *J. Chem. Soc., Perkin Trans.* **1999**, *2*, 493–503.

structure of a peculiar europium complex $[Eu_2\mathbf{L}_2]^{6+}$ shows a relatively selective crystallization of the predominant *M*-enantiomer (87%), which represents an unusual feature of this self-assembly process. The ligand strand with a bidentate binding site does not participate in the coordination but contributes to intermolecular interactions in the solid state. The coordination sphere is thus formed by two tridentate strands provided by two different ligands and completed by three solvent molecules. Photophysical studies performed with the crystalline $[Eu_2\mathbf{L}_2]^{6+}$ qualitatively agree with the site symmetry determined by the X-ray diffraction. However, the solid state structure could not be clearly confirmed by NMR in solution, although the luminescence lifetime in methanol is compatible with three coordinated solvent molecules. In addition to dinuclear complexes, the spectrophotometric, NMR, and ES-MS titrations revealed the formation of the $[Ln_2\mathbf{L}_3]^{6+}$ species. Their exact structure could not be evidenced, but the NMR spectra indicate the presence of low symmetrical complexes in solution. The overall speciation of complexes as the function of $[Ln]_{tot}/[\mathbf{L}]_{tot}$ varies along the Ln(III) series, which seems to be evoked by changes in ionic radius. Differences in the coordination behavior of La(III) and Lu(III) are demonstrated by the NMR titrations. The increasing electrostatic interactions between donor atoms of **L** and Ln(III) cations stabilize $[Ln_2\mathbf{L}_2]^{6+}$ and $[Ln_2\mathbf{L}]^{6+}$ species although the thermodynamic stability constants determined by spectrophotometry do not significantly vary.

It may be concluded that the formation of tripodal monometallic complexes suffers from poor preorganization of **L** because of steric constraints associated with the short spacer between binding sites. The preferred "open" conformation of **L** provides the Ln(III) complexes, which are not suitable for practical sensing applications because of their relatively low thermodynamic stability in solution and for apparent lability of the unsaturated coordination sphere. Nevertheless, the analysis of structural factors obtained for **L** and $[Eu_2\mathbf{L}_2]^{6+}$ allows to improve the ligand design to better control the ligand occupancy of the Ln(III) coordination sphere, for example, by increasing the spacer length of one binding strand.

Experimental Section

Solvents and Starting Materials. These were purchased from Acros Organics, Fluka AG, and Aldrich and used without further purification unless otherwise stated. *N*,*N*-dimethylformamide (DMF), acetonitrile, and dichloromethane were distilled over CaH_2. 1,1,1-(Trisaminomethyl)ethane (TAME) was purchased from Fluka AG or synthesized according to published procedures.[31] The perchlorate salts were prepared from the corresponding oxides (Rhodia and Aldrich, 99.99%) and dried according to published procedures.[32] Ln(III) content of solid salts was determined by complexometric titrations with Titriplex III (Merck) in the presence of urotropine and xylene orange. 6-(*N*,*N*-diethylcarbamoyl)pyridine-2-carboxylic acid was prepared according to published procedures.[13] ***Caution!*** *Perchlorate salts are potentially explosive and should be handled carefully in small quantities.*[33]

Preparation of 1,1-Bis[carbamoyl-6-(*N*,*N*-diethylcarbamoylpyridine-2)methyl]-1-amino-methyl-ethane ($\mathbf{L^1}$). Pyridinedicarboxylic-*N*,*N*-diethylamide (349 mg, 1.57 mmol) was refluxed with CDI (260 mg, 1.6 mmol) in 50 mL of tetrahydrofuran (THF) for 3 h under an inert atmosphere of N_2. This solution was then added dropwise to 1,1,1-(trisaminomethyl)ethane (TAME, 92.6 mg, 0.78 mmol) dissolved in THF (40 mL) under an inert N_2 atmosphere. The mixture was stirred for 20 h at reflux, washed with half-saturated Na_2CO_3, dried over anhydrous Na_2SO_4, and evaporated. The resulting crude compound was dissolved in small volume of HCl (1 M) and washed two times with CH_2Cl_2. The pH of the aqueous phase was adjusted to 10 (KOH, 2 M), and the compound $\mathbf{L^1}$ was extracted by CH_2Cl_2 in 68% yields.

$\mathbf{L^1}$: ^{1}H NMR (CD_3CN): δ = 0.88 (3H, s, CH_3), 1.17 (6H, t, CH_3), 1.26 (6H, t, CH_3), 3.30 (4H, q, CH_2), 3.35 (4H, q, CH_2), 3.56 (4H, q, CH_2), 6.67 (2H, d, CH), 8.05 (2H, t, CH), 8.15 (2H, d, CH), 9.00 (2H, t, NH) ppm. ESMS: m/z = 274.3 $(\mathbf{L^1} + H + Na)^{2+}$, 526.1 $(\mathbf{L^1} + H)^+$.

Preparation of 1,1-Bis[carbamoyl-6-(*N*,*N*-diethylcarbamoylpyridine-2)methyl]-1-mono[carbamoyl-6-(methylpyridine-2)-methyl]ethane (L). 6-Methylpyridine-2-carboxylic acid (180 mg, 1.31 mmol) was refluxed with CDI (243 mg, 1.5 mmol) in 30 mL of THF for 3 h under inert atmosphere of N_2. This solution was then added to the solution of $\mathbf{L^1}$ (277 mg, 0.53 mmol) in THF. The mixture was refluxed for 20 h, washed with half-saturated NH_4Cl, dried over anhydrous Na_2SO_4, and evaporated. The resulting crude compound was purified by column chromatography (silica gel, CH_2Cl_2−CH_3OH 97.5:2.5) and recrystallized from acetonitrile to afford **L** as a white solid (64% yields).

L: ^{1}H NMR (CD_3CN): δ = 0.95 (3H, s, CH_3), 1.18 (6H, t, CH_3), 1.28 (6H, t, CH_3), 2.62 (3H, s, CH_3), 3.31 (6H, m, CH_2), 3.38 (4H, q, CH_2), 3.58 (4H, q, CH_2), 7.43 (1H, d, CH), 7.67 (2H, d, CH), 7.84 (1H, t, CH), 7.94 (1H, d, CH_2), 8.06 (2H, t, CH_2), 8.20 (2H, d, CH_2), 9.06 (3H, t, NH) ppm. ESMS: m/z = 645.1 $(\mathbf{L} + H)^+$, 667.5 $(\mathbf{L} + Na)^+$.

Crystal Data of the $C_{34}H_{44}N_8O_5\cdot H_2O$ (L). (*diffraction data are weak*): M = 660.77, triclinic, space group $P\bar{1}$, a = 9.5730(11) Å, b = 12.8128(15) Å, c = 15.5018(18) Å, α = 83.771(9), β = 84.412(9), γ = 73.686(9), V = 1809.6(4) Å^3, Z = 2, λ = 0.7107 Å, T = 293 K, μ = 0.085 mm^{-1}, 37127 reflections measured of which 8329 were unique and 3317 were observed ($I/\sigma > 2$), 442 parameters refined, R = 0.0749 and ωR = 0.0747 ($I/\sigma > 2$).

Preparation and Isolation of $[Eu_2\mathbf{L}_2](ClO_4)_6\cdot xH_2O$. A solution of $Eu(ClO_4)_3\cdot xH_2O$ (0.016 mmol) in acetonitrile (400 μL) was added to a solution of **L** (0.016 mmol) in acetonitrile (400 μL) under stirring. The complex precipitates at room temperature under diffusion of *tert*-butylmethylether. The resulting white powders were collected, washed with *tert*-butylmethylether, and dried. The complex was recrystallized from its methanolic solution with 1 drop of acetonitrile by diffusion of *tert*-butylmethylether, the crystals collected by filtration, and dried under vacuum for 5 h to give the europium complex in 64% yield with respect to **L**. Anal. Calcd for $[Eu_2(C_{34}H_{44}N_8O_5)_2](ClO_4)_6\cdot 1CH_3OH\cdot 12H_2O$ (**1**): C, 33.98; N, 9.14; H, 4.74. Found: C, 33.97; N, 9.19; H, 4.80%.

Crystal Data of $[Eu_2(C_{34}H_{44}N_8O_5)_2(CH_3OH)_6](ClO_4)_6\cdot 5CH_3OH$. M = 2542.9, orthorhombic, space group $P2_12_12_1$, a = 14.4386(7) (Å), b = 21.9512(8) (Å), c = 35.3158(16) (Å), α = β = γ = 90°, V = 11193.1(8) (Å^3), D_c = 1.509 gcm^{-1}, μ = 1.344 mm^{-1}, Z = 4, λ = 0.7107 Å, T = 150 K, 96437 reflections collected, 15891 reflections independent (R_{int} = 0.046) and 11048 observed reflections [$F_0 > 4\sigma(F_0)$], 1171 refined parameters, R = 0.056, ωR = 0.055.

Spectroscopic and Analytical Measurements. ^{1}H NMR spectra were recorded on high-field NMR spectrometer (400 MHz, Bruker). Electronic spectra in the UV−vis were recorded from acetonitrile solutions with a Perkin-Elmer Lambda 900 spectrometer using quartz cells of 0.1 path length. Mathematical

(31) (a) Geue, R. J.; Searle, G. H. *Aust. J. Chem.* **1983**, *36*, 927–935. (b) Brown, K. N.; Hockless, C. R.; Sargeson, A. M. *Dalton Trans.* **1999**, 2171–2175.

(32) Desreux, J. F. In *Lanthanide Probes in Life, Chemical and Earth Sciences*; Bünzli, J.-C. G., Choppin, G. R., Eds.; Elsevier: Amsterdam, 1989; Chapter 2.

(33) Raymond, K. N. *Chem. Eng. News* **1983**, *61*, 4.

treatment of the spectrophotometric titrations was performed with the SPECFIT program.[34] Routine ESMS spectra were measured with a API 150EX LC/MS system. Pneumatically assisted electrospray (ESI-MS) mass spectra were recorded from 10^{-4} M acetonitrile solutions of Ln(III) complexes on a Finnigan SSQ7000 instrument with the optimized ionization temperature (150 °C) or on API III Applied Biosystem (ISV 3500 V/OR 30 V). Luminescence spectra and decays in solution were recorded on Perkin-Elmer LS-50 spectrometer. Emission and excitation spectra of solid samples were measured on a Horiba Fluorolog 3 instrument with the excitation wavelength 270 nm and with different emission wavelengths. To avoid second order light from the excitation wavelength, we used a cutoff filter at 536 nm. Luminescence lifetimes were measured by exciting the solid samples at 355 nm with a pulsed Nd:YAG laser (Quantel Brilliant, 7 ns pulse width). The measuring time corresponds to the deactivation time of the sample. The obtained signal was then integrated. The system used for detection consisted of a Spex 270 M monochromator, a Hamamatsu photomultiplier, and a Stanford research systems SR 400 photon counter. The crystallographic data were collected at 150 K on a Stoe IPDS diffractometer with graphite monochromated Mo[Kα] radiation (λ = 0.7107 Å). The structure was solved by direct methods (SIR97),[35] all other calculations were performed with XTAL program package.[36]

Acknowledgment. We gratefully acknowledge the support of this work by the University of Geneva, the Swiss National Science Foundation, and the COST D38 Action. We thank Philippe Perottet and Nathalie Oudry for recording ESMS spectra, Dr. Tiphaine Penhouet for measuring some emission spectra and Prof. A. Hauser for providing access to spectroscopy equipment. Dr Céline Besnard is acknowledged for the X-ray measurement and the structure refinement of **L**.

Supporting Information Available: Tables with H−bond lengths in **L**, selected bond lengths in $[Eu_2\mathbf{L}_2]^{6+}$ and f−f transitions. Figures showing the crystallographic structure of **L** and $[Eu_2\mathbf{L}_2]^{6+}$, NMR of isolated compounds, NMR titrations with Lu(III) and La(III), distribution curves according to the NMR titration, assignment of protons for the Lu(III) complexes, VT-NMR spectra, ESMS spectra, fitted spectra from the spectrophotometric titration with Tb(III) and distribution curves, emission and excitation spectra, models of possible arrangements within Eu(III) complexes. This material is available free of charge via the Internet at http://pubs.acs.org.

(34) Gampp, H.; Maeder, M.; Meyer, C. J.; Zuberbuehler, A. D. *Talanta* **1986**, *33*(12), 943–951.

(35) Altomare, A.; Burla, M. C.; Camalli, M.; Cascarano, G.; Giacovazzo, C.; Guagliardi, A.; Moliterni, A. G. G.; Polidori, G.; Spagna, R. *J. Appl. Crystallogr.* **1999**, *32*, 115–119.

(36) *XTAL 3.2 User's Manual*; Hall, S. R.; Flack, H. D.; Stewart, J. M., Eds.; Universities of Western Australia, Geneva, and Maryland; 1992.